Environment International 163 (2022) 107173

Contents lists available at ScienceDirect

Environment International

journal homepage: www.elsevier.com/locate/envint

Nanoplastics affect the inflammatory cytokine release by primary human monocytes and dendritic cells

Annkatrin Weber [a], Anja Schwiebs [b], Helene Solhaug [c], Jørgen Stenvik [c,d], Asbjørn M. Nilsen [c], Martin Wagner [e,*], Borna Relja [f,1], Heinfried H. Radeke [b,1]

[a] Goethe University, Department of Aquatic Ecotoxicology, Faculty of Biological Sciences, Max-von-Laue-Straße 13, 60438 Frankfurt am Main, Germany
[b] Goethe University Hospital, Institute of General Pharmacology and Toxicology, pharmazentrum frankfurt, Theodor-Stern-Kai 7/75, 60596 Frankfurt am Main, Germany
[c] Norwegian University of Science and Technology, Department of Clinical and Molecular Medicine, Faculty of Medicine and Health Sciences, Erling Skjalgssons gate 1, Trondheim, Norway
[d] Norwegian University of Science and Technology, Centre of Molecular Inflammation Research, Olav Kyrres gate 17, Trondheim, Norway
[e] Norwegian University of Science and Technology, Department of Biology, Høgskoleringen 5, Realfagbygget, 7491 Trondheim, Norway
[f] Otto-von-Guericke University, Department of Radiology and Nuclear Medicine, Experimental Radiology, Leipziger Str. 44, 39120 Magdeburg, Germany

ARTICLE INFO

Handling Editor: Adrian Covaci

Keywords:
Microplastic
Nanoplastic
Particle toxicity
Plastics
Plastic pollution

ABSTRACT

So far, the human health impacts of nano- and microplastics are poorly understood. Thus, we investigated whether nanoplastics exposure induces inflammatory processes in primary human monocytes and monocyte-derived dendritic cells. We exposed these cells *in vitro* to nanoplastics of different shapes (irregular vs. spherical), sizes (50–310 nm and polydisperse mixtures) and polymer types (polystyrene; polymethyl methacrylate; polyvinyl chloride, PVC) using concentrations of 30–300 particles cell^{-1}. Our results show that irregular PVC particles induce the strongest cytokine release of these nanoplastics. Irregular polystyrene triggered a significantly higher pro-inflammatory response compared to spherical nanoplastics. The contribution of chemicals leaching from the particles was minor. The effects were concentration-dependent but varied markedly between cell donors. We conclude that nanoplastics exposure can provoke human immune cells to secrete cytokines as key initiators of inflammation. This response is specific to certain polymers (PVC) and particle shapes (fragments). Accordingly, nanoplastics cannot be considered one homogenous entity when assessing their health implications and the use of spherical polystyrene nanoplastics may underestimate their inflammatory effects.

1. Introduction

Plastic pollution in one very visible indicator of the Anthropocene (Kramm et al., 2018). Plastic debris accumulates in natural environments on a global scale and fragments into micrometer-sized particles, microplastics (1–1,000 μm, Hartmann et al., 2019). Even smaller plastic particles, nanoplastics (NP, 1–1,000 nm), form during plastic degradation but have rarely been detected in the environment or biota due to methodological limitations (Lambert & Wagner, 2016; Wagner & Reemtsma, 2019). However, international institutions and researchers have voiced concern over the potential health impacts, in particular of NP, but conclude that exposure and toxicity data are scarce if existent at all (SAPEA, Science Advice for Policy by European Academies, 2018; Norwegian Scientific Committee for Food and Environment [VKM], 2019).

Provided their presence in foodstuff and air, human exposure to microplastics may be widespread and can range from 74,000 to 121,000 particles per person per year (Barboza et al., 2018; Cox et al., 2019; Dris et al., 2017). For NP, currently no quantitative exposure estimates exist but based on the assumption that plastics further fragment into smaller particles, human exposure to NP might be higher than for microplastics. The principal exposure routes are ingestion (foodstuff, beverages, drinking water), inhalation (air, dust) and dermal uptake (e.g., via personal care products) of NP emitted to the environment (Kawecki & Nowack, 2019). Likewise, it remains unknown how NP exposure translates to internal concentrations.

* Corresponding author.
E-mail address: martin.wagner@ntnu.no (M. Wagner).
[1] Both authors contributed equally to this work.

https://doi.org/10.1016/j.envint.2022.107173
Received 14 December 2021; Received in revised form 13 February 2022; Accepted 3 March 2022
Available online 15 March 2022

One central idea is that very small plastic particles can transfer across biological barriers and infiltrate tissues (Wright & Kelly, 2017). For instance, polystyrene (PS) spheres ≤ 6 μm pass the intestinal wall of rodents and translocate into lymph nodes (Carr et al., 1996). In rats and dogs, 1.3, 3 and 7 μm microspheres can translocate from the lung into associated lymph nodes through macrophage-dependent transport (Harmsen et al., 1985; Snipes et al., 1984). A dermal uptake of NP appears to be limited although few studies have reported a transfer of PS spheres ≤ 500 nm (Kohli & Alpar, 2004; Mahe et al., 2009).

Another central idea is that exposure to small plastic particles induces inflammation. Occupational health research on workers from textile and plastics industries as well as orthopedic research on the release of plastic particles from implants supports this idea (Goodman & Lidgren, 1992; Prata, 2018). Further, *in vitro* studies have demonstrated that immune cells respond to NP and microplastics exposures (reviewed in Danopoulos et al., 2021). Here, plastic particles stimulated the release of pro-inflammatory cytokines, for instance, in peripheral blood mononuclear cells (PBMCs) and macrophages *in vitro* (González et al., 1996; Han et al., 2020; Hwang et al., 2020; Matthews et al., 2000).

However, limited research has been performed on the effects of NP on human monocytes (MOs) and monocyte-derived dendritic cells (moDCs, Shanbhag et al., 1995). Both cell types function as precursor and effector cells, survey peripheral tissues and maintain endothelial integrity (Teh et al., 2019). Upon an inflammatory stimulus, MOs circulating in the blood stream migrate into tissues and differentiate into either macrophages or DCs (Teh et al., 2019). DCs link innate and adaptive immune responses and modulate T cell development, differentiation and functions (Waisman et al., 2017). MOs and moDCs release pro-inflammatory or anti-inflammatory cytokines that activate or suppress inflammation, respectively.

While some knowledge on the inflammatory effects of specific plastics exists (mainly from implant abrasion), humans will be exposed to a heterogeneous mixture of NP and microplastics that varies, amongst others, regarding the polymer type as well as the size and shape of the particles. Since comparative data is missing, the aim of our study is to characterize the effects of NP with different physico-chemical properties on the cytokine release of human MOs and immature moDCs. We used these cell types because they are underrepresented with regards to particle toxicity compared to others (e.g., macrophages). As endpoints, we determined the release of pro-inflammatory IL-6, TNF, IL-12p70 and IL-23 and anti-inflammatory IL-10 as key mediators of inflammation (see S1.1 for function of these cytokines).

We exposed the cells to irregular, polydisperse PS ($PS_{polyd.}$), polymethyl methacrylate ($PMMA_{polyd.}$) and polyvinyl chloride ($PVC_{polyd.}$) particles (<600 nm) as well as uniform 50, 100 and 310 nm PS nanospheres. We selected these to cover three polymers commonly used in *in vitro* toxicity studies (PS) and orthopedic research (PMMA) as well as one polymer with a high potential for chemical toxicity (PVC, Zimmermann et al., 2019). In addition, this setup allows us to assess the impact of particle size (50, 100 and 310 nm PS spheres) and shape (irregular vs. spherical PS). Importantly, we also analyzed the effects of NP leachates to compare physical and chemical impacts. Further, we determined the particle toxicity in presence of lipopolysaccharides (LPS) as immune stimulus simulating a bacterial infection. This addresses the question of whether NP exposure modulates the responsiveness of immune cells that were activated by an endotoxin stimulus.

2. Materials and methods

2.1. Ethics statement

PBMCs were isolated from buffy coats drawn from anonymous healthy blood donors by the blood donation center DRK-Blutspendedienst Baden-Württemberg-Hessen, Institut für Transfusionsmedizin und Immunhämatologie Frankfurt am Main, Frankfurt, Germany. Prior to blood sampling, all participants routinely gave written informed consent. According to the institutional ethics committee of the Goethe University Hospital, Frankfurt, Germany and local legislation, an additional consent concerning the here presented experiments is not required, as the buffy coats were used anonymously for *in vitro* assays with no link to patient data.

2.2. Preparation and stimulation of human MOs and immature moDCs

MOs and moDCs were obtained from the PBMC fraction in human buffy coats. Briefly, PBMCs were isolated by gradient density centrifugation (d = 1.077 g mL^{-1}) with either Histopaque–1077 (Sigma–Aldrich, Darmstadt, Germany) or Biocoll (Biochrom, Darmstadt, Germany). Cells were washed twice with phosphate-buffered saline (PBS, w/o Mg^{2+} and Ca^{2+}).

MOs were separated from the remaining PBMCs by resuspending the cells in RPMI 1640 with supplements and 20 % FCS and seeding them into 12-well plates (3.8 cm^2 $well^{-1}$, 7,600,000 cells in 600 μL medium per well). After 1 h of incubation at 37 °C and 5 % CO_2, cells were washed three times with medium (RPMI 1640 with supplements and 10 % FCS) to remove nonadherent cells. All remaining, adherent cells (approximately 866,000 ± 318,000 (SD) cells $well^{-1}$, cultured in 600 μL RPMI 1640 with 10 % FCS) were assumed to be MOs and used directly for the experiments.

For moDC differentiation, MOs were grown for 7 d in cell culture flasks with 30 mL RPMI 1640 with supplements and 10 % heat-inactivated serum containing human IL4 (10 ng mL^{-1}, MACS Miltenyi Biotec, Bergisch Gladbach, Germany), recombinant human GMCSF (8 ng mL^{-1}, PeproTech, Hamburg, Germany) and ciprofloxacin (3.3 μg mL^{-1}, Cayman, Ann Arbor, MI, US). After the differentiation, immature moDCs were scraped, resuspended in serum-free medium and seeded in 6-well plates (9.6 cm^2, 750,000 cells in 1,200 μL of medium per well). Plates were incubated for 1 h at 37 °C and 5 % CO_2 and directly used for the experiments (further details on cell culturing in S2.1).

We used FACS (FACS Canto II, BD Biosciences, Heidelberg, Germany) to verify the purity of MOs and the immature moDCs by determining the expression of cell type–specific surface markers (MOs: CD14, CD16, immature moDCs: CD11b, CD11c, DCIR, MHC2, methodological details and results in S2.7 and S3.4).

2.3. Nanoplastics preparation

Non-functionalized 50 and 100 nm PS latex nanospheres (PS_{50}, PS_{100}) were purchased from Polysciences Europe (Polybead, 08691–10, 00876–15, Hirschberg an der Bergstrasse, Germany). Non-functionalized, red fluorescent 310 nm PS latex nanospheres (PS_{310}) were obtained from Magsphere (PSF-300NM, Pasadena, CA, USA). We removed the liquid from the suspensions to avoid impacts of biocides and other chemicals potentially present in the liquid phase. The nanospheres were separated from the solvent via centrifugation, washed twice with ultrapure water and resuspended in physiological saline (154 mmol NaCl). Originally, we also intended to use 1 μm PS spheres in our study. These microspheres did, however, fragment during the solvent removal (Fig. S2) and could not be used.

Polydisperse (polyd.) PVC powder (irregular shape, < 50 μm) was purchased from PyroPowders (Erfurt, Germany). Irregular polydisperse PMMA (green, fluorescent) and PS particles (orange) were produced by cryomilling from household products (details and SEM images in S2.2). We isolated the size fraction ≤ 5 μm by suspending the PMMA, PS and PVC powders in 1.5 mL ultrapure water. After sonication (15 min, 215 W), larger particles were allowed to settle for 10–25 min. The supernatant containing the nanosized fraction was separated and lyophilized to remove the water. This process was repeated multiple times to produce sufficient amounts of particles. The resulting NP fraction was resuspended in 1 mL physiological saline ($PMMA_{polyd.}$, $PS_{polyd.}$, $PVC_{polyd.}$). The surfactant Tween 20 (1:10,000 v/v), Sigma-Aldrich, Darmstadt, Germany) was added to the $PS_{polyd.}$ suspension to avoid

agglomeration. The use of Tween 20 at concentrations of 3.7×10^{-5} % (v/v, MOs) and 6.25×10^{-6} % (moDCs) did not significantly affect cytokine production ($p > 0.05$, unpaired *t*-test (control vs. $PS_{polyd.}$ control (=Tween 20 control)), raw data in S3.9).

As controls, we prepared a physiological saline without particles (control) and a physiological saline with Tween 20 ($PS_{polyd.}$ control). Due to the presence of non-identifiable chemicals in the polymers (see 2.4), we further prepared leachates from the $PMMA_{polyd.}$, $PS_{polyd.}$ and $PVC_{polyd.}$ particles to differentiate between physical and chemical toxicity. For leachate preparation, particle stock suspensions were stored at 5 °C for six weeks, before 500 µL of each were centrifuged three times (21,130 g) for 270 min and the particle-free supernatant was removed ($PMMA_{leach}$, PS_{leach}, PVC_{leach}, S2.2, NTA results in Fig. S7). In total, our study included eleven NP suspensions and leachates (control, $PS_{polyd.}$ control, $PMMA_{polyd.}$, $PS_{polyd.}$, $PVC_{polyd.}$, $PMMA_{leach}$, PS_{leach}, PVC_{leach}, PS_{50}, PS_{100}, PS_{310}). Further details on the preparation of the stock suspensions are included in S2.2.

2.4. Polymer types and chemical content

The polymer type of the plastic powders was analyzed with Attenuated total reflection Fourier-transform infrared spectroscopy (ATR-FTIR, Spectrum Two, Perkin Elmer, Waltham, MA, USA). ATR-FTIR results confirmed the polymer types PMMA, PS and PVC for the plastic powders (full methods and results in S2.3 and S3.1).

The chemical content of the plastic powders was analyzed using Pyrolysis-gas chromatography-mass spectrometry (py-GC–MS) on a Multi–Shot Pyrolyzer and Auto–Shot sampler (Frontier–Laboratories, Saikon, Japan) attached to an Agilent 7890B gas chromatograph and an Agilent 5977B Mass Selective Detector (Agilent, Santa Clara, CA, USA). The detected pyrolysis compounds resulting from plastic polymer pyrolysis were compared to the NIST 2011 Mass Spectral Library to conclude on potential chemical compounds originally included in the plastic polymers. In total, quantities of pyrolysis products were low compared to other plastic samples (Zimmermann et al., 2019) indicating limited additive content in our plastic particles. According to the NIST analysis, detected pyrolysis products could not be matched to chemicals commonly used in polymer industry and the chemicals compounds in the PS, PMMA and PVC plastic therefore remain unknown (full methods and results in S2.4 and S3.2).

2.5. Particle concentration, size distribution and settling velocity

Particle size distributions were determined for all stock suspensions by nanoparticle tracking analysis (NTA) using a NanoSight LM10 instrument (Malvern Panalytical, Almelo, Netherlands, detection range: 50–2,000 nm). For NTA, particle stock solutions were diluted in ultrapure water and vortexed intensively to avoid agglomeration during the measurement. We used the NTA results to determine particle concentrations in the suspensions and corrected those with the results from the corresponding particle-free controls. All suspensions were diluted to 10^{10} particles mL^{-1} with physiological saline. Leachates and the $PS_{polyd.}$ control were diluted in the same way (further details on NTA in S2.5).

Further, we theoretically calculated mean settling velocity of the six particle types according to Stokes' law (Hinderliter et al., 2010) based on (geometric) mean particle diameter, polymer density (PS: 1.09 g cm^{-3}, PMMA: 1.18 g cm^{-3}, PVC: 1.40 g cm^{-3}) as well as RPMI 1640 density (1.006 g cm^{-3}, according to Thermo Fisher Scientific) and dynamic viscosity (0.79 mPa × s, Rinker et al., 2001). From settling velocities, we determined the percentage of particles settling in the wells within 18 h of exposure.

2.6. Exposure of moDCs and MOs to nanoplastics

MOs and immature moDCs were exposed to the NP suspensions or leachates for 18 h at 37 °C and 5 % CO_2, both in absence and presence of lipopolysaccharides (LPS, *E. coli* O127:B8, Sigma Aldrich, Darmstadt, Germany). In total, we repeated the experiments with moDCs five times and with MOs six times, using cells from different buffy coats (i.e., different donors) for each experiment. MOs and moDCs were exposed to 300 particles $cell^{-1}$ (4.56×10^8 particles mL^{-1}) and 100 particles $cell^{-1}$ (7.5×10^7 particles mL^{-1}), respectively (particles $cell^{-1}$ concentrations = number of particles per well / number of MOs or moDCs per well). We also estimated the corresponding concentrations regarding the mass, volume and surface area (Tab. S2). The lower concentration of NP for moDCs was selected because of their higher sensitivity to immune stimuli.

LPS stimulation was applied cell-specifically. LPS concentrations of 50 ng mL^{-1} (IL-6, TNF, IL-10) and 1 µg mL^{-1} (IL-12, IL-23) for the moDCs exposure were selected based on previous reports (Arlt et al., 2014, Tada et al., 2008). At 50 ng mL^{-1}, IL-6, TNF and IL-10 secretion of dendritic cells is not yet maximal (Tada et al., 2008) allowing both up- and downregulation by NP exposure. MOs were stimulated with 10 µg mL^{-1} LPS. Additional concentration–response experiments show that MOs respond to LPS concentrations lower and higher than 10 µg mL^{-1} (S3.5). For TNF and IL-10, results indicate that MOs had not yet been maximal stimulated at the applied exposure concentration of 10 µg mL^{-1}. For IL-6, no change in cytokine secretion was seen between 0.01 and 100 µg mL^{-1} suggesting maximal stimulation at LPS concentrations < 10 ng mL^{-1}. Thus, all three tested cytokines could be downregulated, while upregulation in MOs was only possible for TNF and IL-10.

Prior to adding the particles to the wells, all stock suspensions were vortexed to reduce particle agglomeration. After transferring the particles (and LPS) to the wells, the plates were thoroughly shaken to distribute the particles homogenously in the wells. The exposure time (18 h) was chosen according to the release kinetics of the cytokines. Based on the study by Waal Malefyt et al. (1991), IL-6, TNF and IL-10 release is maximal within the first 20 h of exposure and exposure time was, thus, set to 18 h. Afterwards, cells in each well were scraped, transferred into precooled reaction tubes and supernatants separated from cells by centrifugation (13,680 g). Supernatants were directly frozen at −80 °C until being analyzed. In addition, 5 µL of the cell suspension was retained after the scrapping and mixed with 5 µL trypan blue solution (0.4 %). Cell number and viability were determined using Neubauer (improved) counting chamber.

The concentrations of IL-6, TNF and IL-10 (both cell types) as well as IL-12p70 and IL–23 (moDCs) in the supernatants were analyzed by ELISA assays (R&D Systems, BioTechne, Wiesbaden–Nordenstadt, Germany) according to the manufacturer's instructions. Due to a limited supernatant volume, IL-10 and IL–12p70 concentrations were only determined for three of the five experiments with moDCs (further details on cell exposure in S2.6).

Due to the pronounced effects of $PVC_{polyd.}$ on MOs in this first series of experiments, we performed a follow-up experiment in which we tested their concentration-dependent effects. MOs from three buffy coats were exposed to $PVC_{polyd.}$ at concentrations of 0, 30, 75, 150 and 300 particles $cell^{-1}$ as described above. The experiments were performed in parallel to avoid inter-day variability. The other particle types were not included as they produced only limited toxicity in the first experiments and we, thus, expected no effects at lower concentrations.

2.7. Confocal microscopy

We characterized cell-particle interactions by exposing immature moDCs to $PMMA_{polyd.}$ and PS_{310} particles and imaging the cells using confocal laser scanning microscopy. We did not image the cells exposed to other NP because these were either not fluorescent ($PS_{polyd.}$, $PVC_{polyd.}$) or too small (PS_{50}, PS_{100}). Differentiated moDCs were seeded into uncoated 8-well µslides (Ibidi, Martinsried, Germany, 250,000 cells in 250 µL medium) and stimulated with particles as described in 2.6. Afterwards, cells were fixed with formaldehyde (AppliChem, Darmstadt, Germany), incubated with Triton X-100 (Sigma-Aldrich/Merck,

Darmstadt, Germany, 0.5 % in PBS) and 5 % milk (skim milk powder (Sigma-Aldrich, Darmstadt, Germany) in TBST (0.1 % (m/v) Tris ultrapure (AppliChem, Darmstadt, Germany) in PBS and 0.1 % Tween 20 (Sigma-Aldrich, Darmstadt, Germany) and finally stained with DAPI for DNA (2 μg mL^{-1}, ERTracker Blue-White DPX, product no.: E12353, Invitrogen, Darmstadt, Germany) and (in case of $PMMA_{polyd.}$ particles) with Alexa Fluor 568 Phalloidin for actin (2 U mL^{-1}, catalog no.: A12380, Invitrogen, Darmstadt, Germany). In between the staining steps, cells were washed with warm PBS. Imaging of the cells was performed with a Zeiss LSM510 Meta system equipped with an inverted Observer Z1 microscope and a Plan-Apochromat 63 × /1.4 oil immersion objective (Carl Zeiss MicroImaging, Göttingen, Germany, more methodological details on confocal microscopy in S2.8). PS_{310} nanospheres were red fluorescent and $PMMA_{polyd.}$ particles were green fluorescent. We applied a red to green color change to the PS_{310} images using Adobe Photoshop (CS5.1) to facilitate the comparison of PS_{310} and $PMMA_{polyd.}$ particles.

2.8. Data analysis and statistics

Absolute cytokine concentrations (data in S3.9) in the exposures of both MOs and moDCs varied intensively between the experiments (i.e., individual buffy coats). Therefore, we normalized cytokine concentrations to the control of the corresponding buffy coat (control = 1). The $PS_{polyd.}$ treatment corresponds to the "$PS_{polyd.}$ control" while all other exposures refer to the "control".

Statistical differences between the treatments were determined using Kruskal-Wallis tests with Dunn's posttest in GraphPad Prism (version 7.04). Concentration-response relationships for $PVC_{polyd.}$ were fitted using a lognormal function and used to interpolate the particle concentration at which cytokine concentrations had doubled compared to control (EC_{2fold}).

3. Results

3.1. Particle characterization

We prepared polydisperse PMMA ($PMMA_{polyd.}$), PS ($PS_{polyd.}$) and PVC ($PVC_{polyd.}$) NP with an irregular shape by cryomilling. According to the NTA, their size distribution ranges from < 50–600 nm (Table. 1) and at least 95 % of the particles in the suspensions are < 455 nm. Further, 50 % of the irregular particles are < 210 nm ($PMMA_{polyd.}$), < 140 nm ($PS_{polyd.}$) or < 215 nm ($PVC_{polyd.}$) and the geometric mean was 117 nm ($PS_{polyd.}$), 193 nm ($PMMA_{polyd.}$) and 203 nm ($PVC_{polyd.}$). In the nanosphere suspensions, mean particle sizes are 80.4 nm for PS_{50}, 104.8 nm for PS_{100} and 295.5 nm for PS_{310}. The larger diameter of PS_{50} may either be related to the instrument's detection limit (50 nm) or an agglomeration of the nanospheres.

Further, we calculated the theoretical settling velocity for each NP type according to Stokes' law. The relative proportion of NP settling in the wells and reaching the cells throughout the 18 h exposure is higher for PS_{310} (22.9–28.9 %) compared to PS_{100} (2.4–3.0 %) and PS_{50} (0.6–0.8 %). For irregular NP, settling and, thus, particle exposure is higher for $PVC_{polyd.}$ (46.1–58.2 %) compared to $PMMA_{polyd.}$ (18.4–23.3 %) and $PS_{polyd.}$ particles (3.3–4.1 %).

3.2. Interaction of nanoplastics with moDCs

Confocal imaging of immature moDCs exposed to spherical PS_{310} and irregular $PMMA_{polyd.}$ particles suggests a close interaction with the cells (Fig. 1). Because we removed nonattached NP before imaging, the observed particles are probably internalized by moDCs. This assumption is supported by the results from z-stack imaging (Fig. S11). At the interface of close cell-particle interactions, the actin cytoskeleton is denser (Fig. 1d) which further supports the idea that moDCs incorporate NP. However, the distribution of NPs in the cells differs as PS_{310} spheres distribute homogenously and in close vicinity of the nucleus (Fig. 1b) while $PMMA_{polyd.}$ particles rather cluster (with some clusters having a size up to 8 μm, Fig. 1c, d).

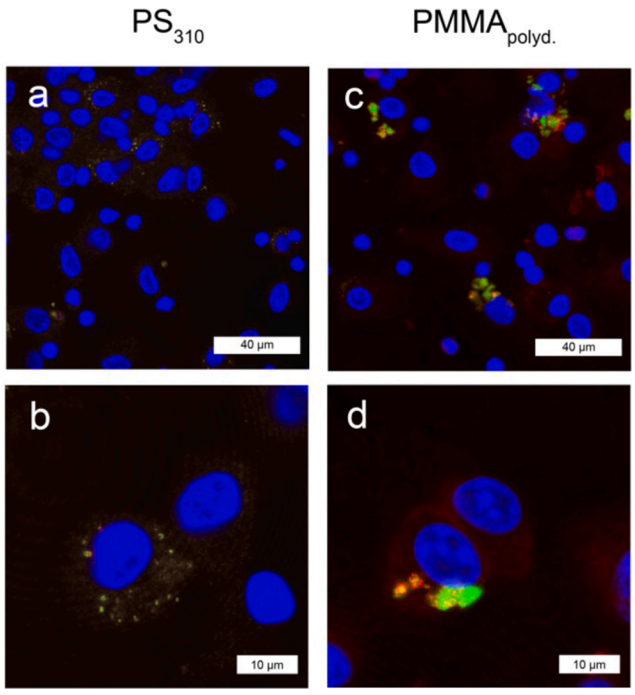

Fig. 1. Interaction of 310 nm PS spheres (a, b) and irregular $PMMA_{polyd.}$ (c, d) with moDCs. Figures a and c were taken at a 63-fold magnification. Figures b and d were further magnified using a crop-factor of 50. Staining: blue = nuclei (DAPI), red (only for $PMMA_{polyd.}$) = actin cytoskeleton (phalloidin), green = nanoplastics. (For interpretation of the references to color in this figure legend, the reader is referred to the web version of this article.)

Table 1
Overview of the nanoplastics characteristics and performed analyses.

Particle type	Particle shape	Particle size [nm]	Cytokines analyzed in moDCs	Cytokines analyzed in MOs	Analysis of NP-cell interactions	Relative proportion of particle settling in the wells [%]
PS_{50}	spherical	80.4 (mean)	IL-6, IL-10, TNF, IL-12p70, IL-23	IL-6, IL-10, TNF	No	0.6–0.8
PS_{100}	spherical	104.8 (mean)			No	2.4–3.0
PS_{310}	spherical	295.5 (mean)			Yes	22.9–28.9
$PS_{polyd.}$	irregular	< 50–600 (mean: 117)			No	3.3–4.1
$PMMA_{polyd.}$	irregular	< 50–600 (mean: 193)			Yes	18.4–23.3
$PVC_{polyd.}$	irregular	< 50–600 (mean: 203)			No	46.1–58.2

3.3. Impact of nanoplastics on cytokine release

The exposure of MOs and moDCs to irregular $PMMA_{polyd.}$, $PS_{polyd.}$ and $PVC_{polyd.}$ NP as well as 50, 100 and 310 nm PS spheres affects the release of cytokines. The effect levels vary between the tested nanoparticles (Fig. 2). The irregular particles induce the strongest changes in IL-6, TNF and IL-10 secretion. In moDCs, they stimulate the release of IL-6 and TNF, while IL-10 remains unaffected. In MOs, irregular $PS_{polyd.}$ and $PVC_{polyd.}$ but not $PMMA_{polyd.}$ particles increase IL-6 and TNF levels. $PMMA_{polyd.}$ and $PVC_{polyd.}$ also increase IL-10 concentrations. In contrast, PS nanospheres inhibit the release of IL-6, TNF and IL-10 except for PS_{50} which slightly stimulates IL-10 release. We also analyzed IL-12p70 and IL-23 secretion in moDCs but concentrations were below the detection limit except for IL-23 in cells co-exposed to LPS (Fig. S12). In the following, we compare effect levels more closely focusing on the polymer type, particle size and shape as well as on the effects of the leachates.

3.3.1. Effects of the polymer type

The polymer type affects the pro- and anti-inflammatory cytokine release. Irregular $PVC_{polyd.}$ particles induce the strongest effects in moDCs and MOs (Fig. 3). In the latter, IL-6, TNF and IL-10 levels are significantly increased compared to control. For moDCs a similar, non-significant tendency is observed for IL-6 and TNF. For $PMMA_{polyd.}$ and $PS_{polyd.}$, a small, non-significant increase was observed for TNF in moDCs ($PMMA_{polyd.}$ and $PS_{polyd.}$) as well as for IL-6 and TNF in MOs ($PS_{polyd.}$). Compared to the other polymer types, $PVC_{polyd.}$ particles induce a more pronounced pro- and anti-inflammatory response, although this is not statistically significant (probably due to a high variability of cytokine levels within the $PVC_{polyd.}$ treatment group).

3.3.2. Effects of leaching chemicals

The $PMMA_{polyd.}$, $PS_{polyd.}$ and $PVC_{polyd.}$ particles used in our study contain low but detectable levels of chemicals (S2.4 and S3.2). As these were detected using pyrolysis GC–MS, they are present in the polymers but not necessarily in the leachates. To compare the physical and chemical toxicity caused by polar chemicals migrating from the NP, we investigated the effects of particle leachates ($PMMA_{leach}$, PS_{leach}, PVC_{leach}). None of the leachates induces a significant cytokine release (Fig. 3). Still, PVC leachates caused a two and threefold increase in IL-6 and TNF in MOs, respectively. However, this induction is 15– and 90-fold lower than the secretion induced by the corresponding $PVC_{polyd.}$ particles. Furthermore, PS leachates induce a two-fold higher IL-6 level compared to control in MOs which, again, is lower than the effects caused by the corresponding particles.

3.3.3. Effects of particle shape and size

In addition to the polymer type, we investigated the effects of different particle shapes and sizes. We included irregular (<50–600 nm) as well as spherical (50, 100, 310 nm) PS NP in our experiments to assess the influence of particle shape on cytokine release. Neither irregular ($PS_{polyd.}$) nor spherical PS particles significantly affect IL-6, TNF and IL-10 secretion in MOs and moDCs compared to the respective controls (Fig. 4). Nevertheless, irregular $PS_{polyd.}$ particles exposure induces a significantly higher IL-6 and TNF release in both cell types compared to PS_{100}. In addition, MOs exposed to $PS_{polyd.}$ also excrete significantly higher IL-6 levels compared to PS_{50} and significantly higher TNF levels compared to PS_{310}. No significant difference between irregular and spherical particles is observed for IL-10. Since the three types of PS nanospheres do not trigger cytokine release, we cannot assess the impact of particle size on cytokine release. Taken together, these results demonstrate that irregular NP induce a stronger release of pro-inflammatory cytokines compared to spherical ones.

3.4. Effects of particle concentration

To investigate the concentration-dependency of cytokine release, we further exposed MOs from three blood donors to 30–300 irregular

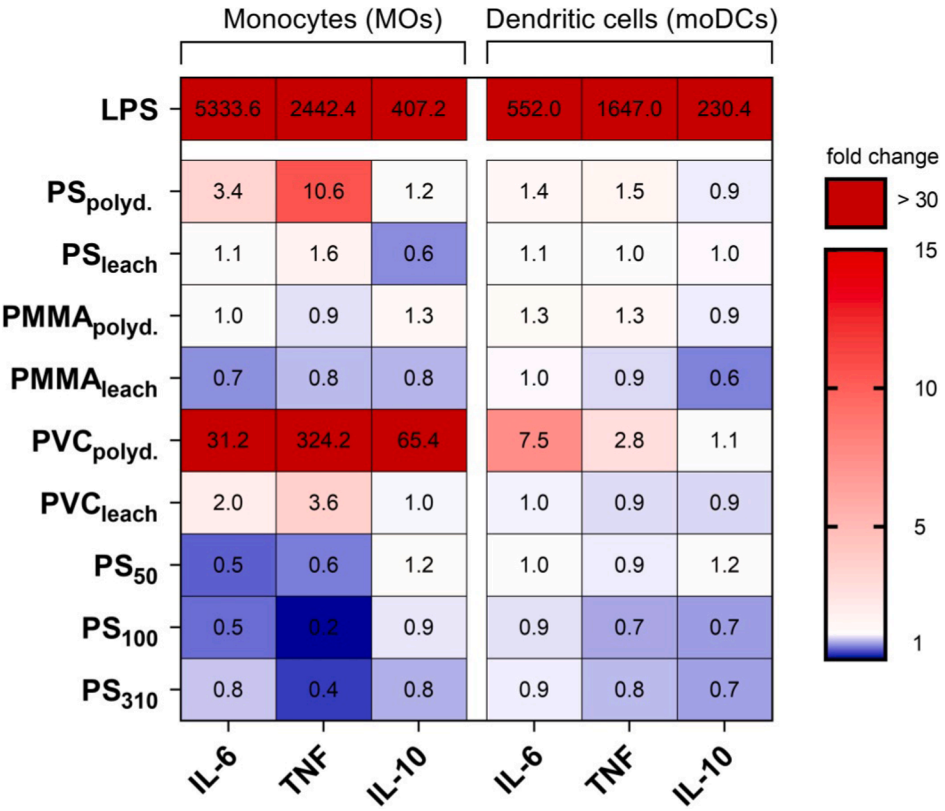

Fig. 2. Cytokine release of human monocytes and dendritic cells exposed to irregular, polydisperse nanoplastics ($PMMA_{polyd.}$, $PS_{polyd.}$, $PVC_{polyd.}$), their respective leachates (leach) and PS nanospheres (50, 100, 310 nm). Monocytes were exposed to 300 particles $cell^{-1}$, dendritic cells were exposed to 100 particles $cell^{-1}$. Relative stimulation (red) or inhibition (blue) was determined as fold change relative to the corresponding control for each buffy coat. The number of experiments was n = 6 for monocytes and n = 5 (IL-6, TNF), n = 3 (IL-10) for dendritic cells. LPS (moDC: 50 ng mL^{-1}, MO: 10 μg mL^{-1}) was used as positive control. (For interpretation of the references to color in this figure legend, the reader is referred to the web version of this article.)

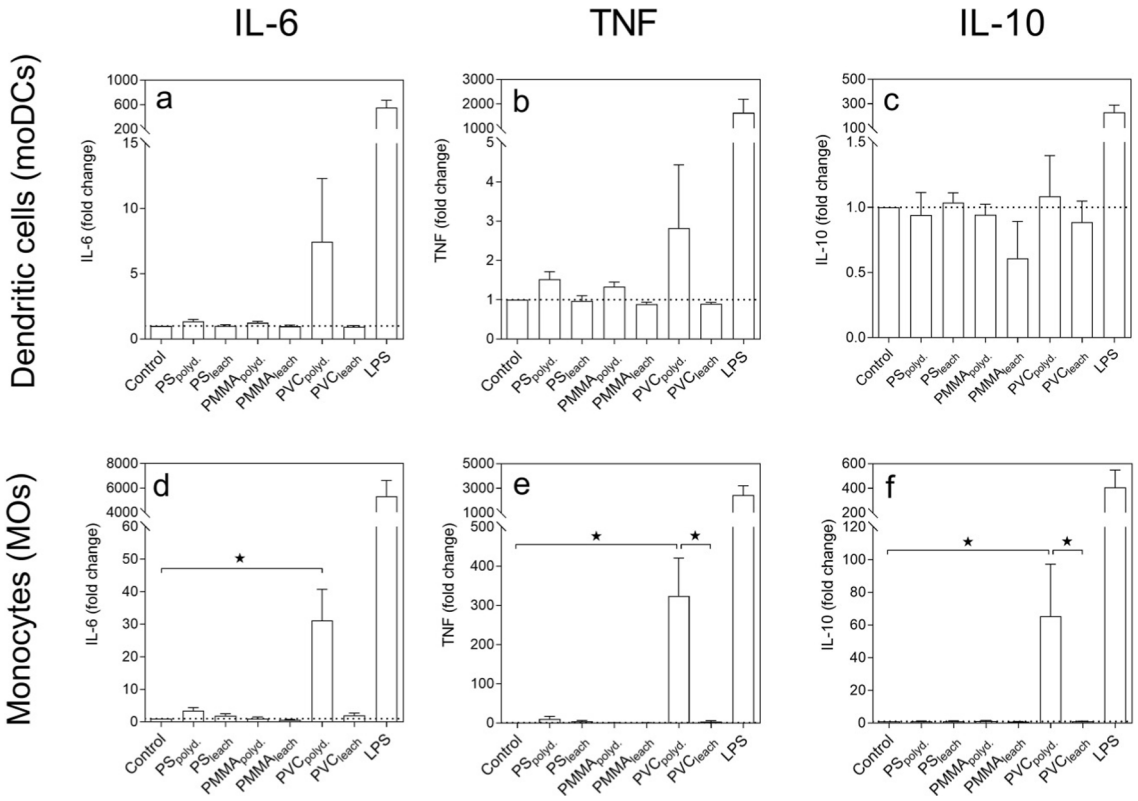

Fig. 3. Cytokine release of human dendritic cells (a–c) and monocytes (d–f) exposed to nanoplastics made of three polymer types. Cytokine concentrations (mean + SEM) were determined in the supernatants of dendritic cells (IL-6, TNF: n = 5; IL-10: n = 3) and monocytes (n = 6) exposed to irregular, polydisperse particles ($PMMA_{polyd.}$, $PS_{polyd.}$, $PVC_{polyd.}$) and their leachates ($PMMA_{leach}$, PS_{leach}, PVC_{leach}). Monocytes were exposed to 300 particles $cell^{-1}$, dendritic cells were exposed to 100 particles $cell^{-1}$. LPS (moDC: 50 ng mL^{-1}, MO: 10 μg mL^{-1}) was used as positive control. Statistical differences were determined between all treatment (except the positive control) using Kruskal-Wallis tests and Dunn's posttests. * $p < 0.05$.

$PVC_{polyd.}$ particles $cell^{-1}$ because these particles induce the strongest effects of all tested NP (see 3.3.1). In all treatments, the secretion of IL-6, TNF and IL-10 increases in a concentration-dependent manner (Fig. 5). Interestingly and in line with the previous experiments, the pro- and anti-inflammatory response varies between the buffy coats, and hence probably donors. At same NP concentrations, MOs of donor 1 are most and those of donor 3 least sensitive. This is in line with the particle concentrations inducing a 2-fold increase in cytokine release ($EC_{2\text{-fold}}$, S3.11).

3.5. Nanoplastic effects in presence of LPS as second stimulus

LPS exposure simulating a bacterial infection causes a strong stimulation of the cytokine release by MOs and moDCs (Figs. 3, 4). Concentration-response experiments with LPS and MOs demonstrate that the response is submaximal for TNF and IL-10 but not for IL-6 (S3.5). An additional NP-induced stimulation, thus, would have been possible at least for TNF and IL-10. However, NP exposure does not further affect the LPS-induced cytokine production of MOs and moDCs compared to the controls (Fig. S12). Hence, NP are not a relevant stimulus for inflammatory cytokine production in presence of the endotoxin LPS.

4. Discussion

4.1. Immune cells internalize nanoplastics

Confocal imaging confirmed that moDCs take up PS_{310} and $PMMA_{polyd.}$. Such uptake of NP is in line with previous research showing that moDCs readily internalize spherical plastic particles, such as 78 nm and 1 μm non-functionalized PS as well as 0.1–15 μm carboxylated PS spheres (Foged et al., 2005; Rothen-Rutishauser et al., 2007). We add to this by demonstrating that moDCs also incorporate irregular plastic particles. Previously, the uptake of irregular particles has only been confirmed for macrophages which phagocytize PMMA cement fragments *in vitro* (Horowitz et al., 1993). Likewise, macrophages incorporated PE and PMMA fragments released by abrasion of prosthetic hip replacements *in vivo* (Schmalzried et al., 1992).

Only a small proportion of the moDCs interacted closely with the NP. This may be a result of the maturation of MOs into moDCs which generally reduces their capacity to internalize particles (Kiama et al., 2001). This suggests, that not only the moDCs, but probably also the MOs used in our study, were in direct contact with both spherical and irregular NP and NP uptake may have been even more pronounced in MOs.

Interestingly, the fluorescence signal of the $PMMA_{polyd.}$ particles clustered in the moDCs with some aggregates being up to 8 μm in size. This size appears to be close to the upper limit for particle uptake by macrophages (Horowitz et al., 1993). Further, in the original stock solutions $PMMA_{polyd.}$ particles had a size of < 600 nm. Hence, we believe that the clusters originate from particle agglomerates. However, we cannot conclude whether particles agglomerated prior or after the internalization by the cells.

4.2. Inflammatory responses to nanoplastics exposure

Out of all tested NP, only $PVC_{polyd.}$ particles induce a significant change in the secretion of both pro- (IL-6, TNF) and anti-inflammatory cytokines (IL-10) in MOs compared to control. The increase of both pro- and anti-inflammatory cytokine levels indicate some counterbalancing mechanism. In a previous study, Trindade et al. (2001) reported that 1 ng IL-10 mL^{-1} suppresses the release of the pro-

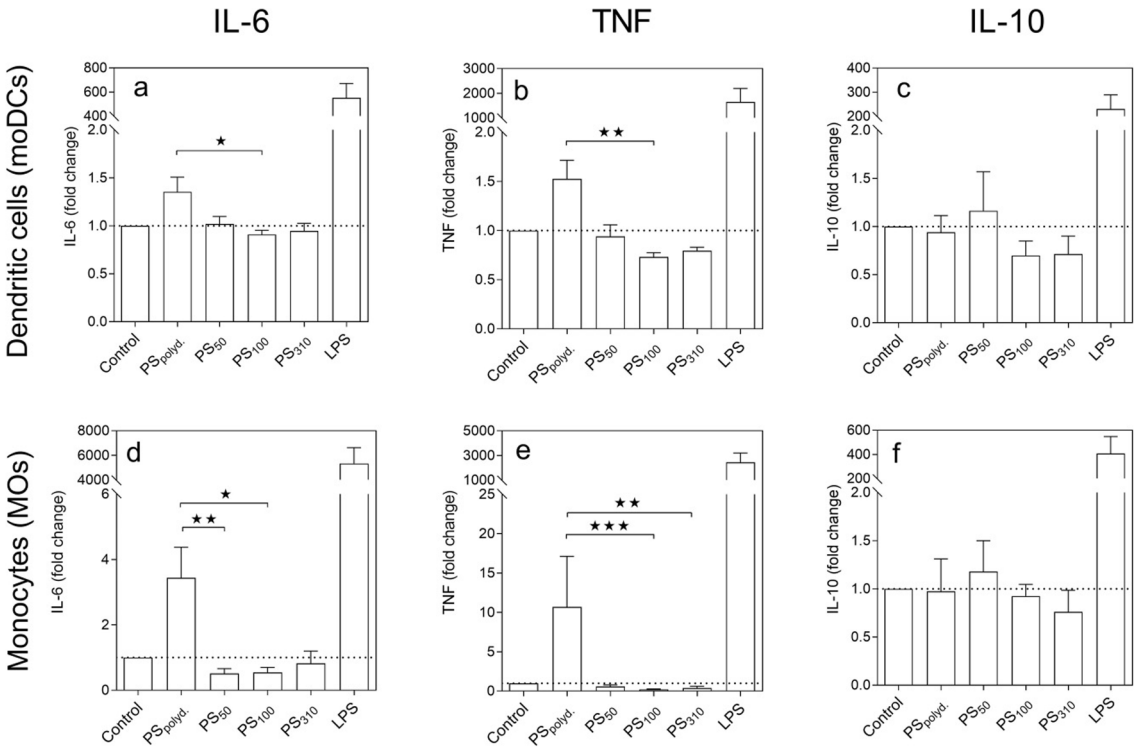

Fig. 4. Cytokine release of human dendritic cells (a–c) and monocytes (d–f) exposed to different sizes and shapes of polystyrene (PS) nanoplastics. Cytokine concentrations were determined in the supernatants of dendritic cells (IL-6, TNF: n = 5; IL-10: n = 3) and MOs (n = 6) exposed to irregular, polydisperse ($PS_{polyd.}$) and spherical PS (50, 100, 310 nm). Monocytes were exposed to 300 particles $cell^{-1}$, dendritic cells were exposed to 100 particles $cell^{-1}$. LPS (moDC: 50 ng mL^{-1}, MO: 10 μg mL^{-1}) was used as positive control. Concentrations were normalized to the corresponding controls (mean + SEM). Statistical differences between all treatments (except the positive control) were determined using Kruskal-Wallis tests and Dunn's posttests. * $p < 0.05$, ** $p < 0.01$, *** $p < 0.001$.

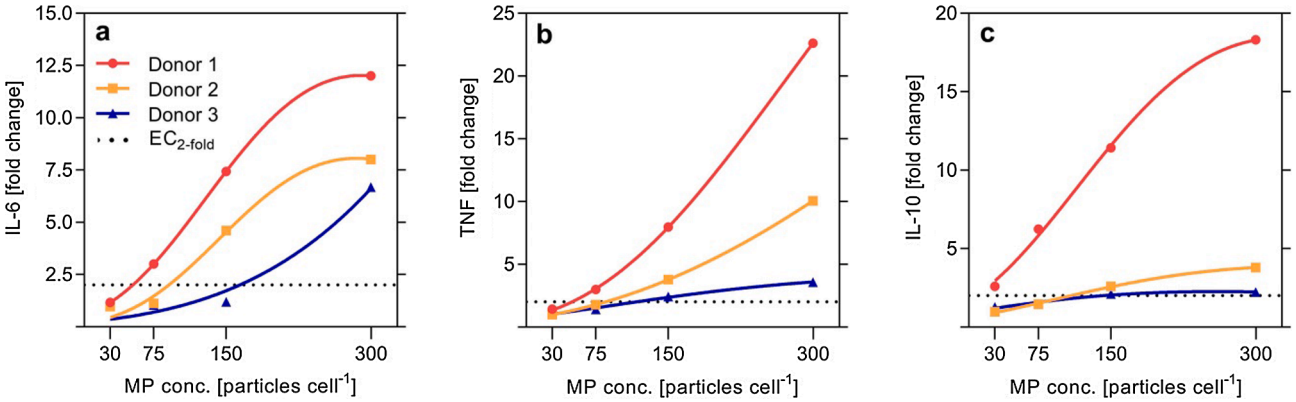

Fig. 5. Cytokine release by human monocytes from three buffy coats (=donors) exposed to irregular PVC nanoplastics ($PVC_{polyd.}$, 30–300 particles $cell^{-1}$). Individual cytokine concentrations are presented as fold change compared to the corresponding control. Dotted line = 2-fold induction. Experiments with the three buffy coats were performed in parallel.

inflammatory IL-6 and TNF in human monocyte-derived macrophages exposed to PMMA particles. In our experiments, MOs exposed to irregular $PVC_{polyd.}$ secret up to 1.6 ng IL–10 mL^{-1}. This suggests at least a partial suppression of pro-inflammatory cytokines and that IL-6 and TNF levels would have been even higher without the counterbalancing effect of IL-10. Unlike this beneficial anti-inflammatory effect, however, high concentrations of IL-10 may also cause inadequate immune suppression and prevent proper infection or cancer control (Huaux, 2018).

In contrast to MOs, moDCs released lower levels of pro-inflammatory cytokines and IL-10 was unaffected by $PVC_{polyd.}$ exposure. This could be due to the lower particle concentrations we used in the moDCs experiments or due to a lower sensitivity of the cells.

To our knowledge, this is the first study investigating the effects of PVC NP on MOs and moDCs. Previous publications have examined PVC effects on cytokine secretion only in cell types other than macrophages, MOs or moDCs: Han et al. (2020) reported that larger irregular PVC microplastics (25–75 μm) induced TNF release in human PBMCs and earlier studies have shown that PVC exposure can induce inflammation *in vivo*. In rats, implanted PVC sheets caused acute and substantial chronic inflammation over 21 d (Marchant et al., 1986). An intratracheal and intraperitoneal exposure to PVC powder resulted in an encapsulation of the particles or an accumulation of macrophages, fibroblasts and giant cells (Pigott & Ishmael, 1979).

In contrast to immune cells exposed to $PVC_{polyd.}$ NP, the effects of $PMMA_{polyd.}$ and $PS_{polyd.}$ on cytokine production are minor and non-significant compared to control. These findings, especially regarding

$PMMA_{polyd.}$ particles, seem to contrast previous *in vitro* studies from orthopedics showing the involvement of PMMA particles in inflammatory processes (Gibon et al., 2017). We believe this difference is a consequence of the limited comparability of studies due to differences in particle size, shapes and concentrations: A major proportion of the relevant literature on *in vitro* effects of PMMA particles on the inflammatory cytokine release of human mononuclear cells and macrophages used PMMA spheres > 1 μm. In addition, studies with smaller PMMA particles applied much higher concentrations than in our study (Chadha et al., 1995; Lind et al., 1998; Nakashima et al., 1999; Trindade et al., 1999, 2001; Wooley et al., 1996). Irregular, polydisperse PMMA particles (0.1–10 μm, 75 % < 0.5 μm) did affect TNF release in human macrophages at concentrations of 100 μm^3 NP volume $cell^{-1}$ (equivalent to 190–24,000 particles $cell^{-1}$ of 100–500 nm PMMA spheres) but not at lower concentrations (Ingham & Fisher, 2000). 325 nm PMMA spheres significantly enhanced IL-6 but not TNF release in human monocyte-derived macrophages at 500,000 particles $cell^{-1}$ but not at lower concentrations (González et al., 1996). In line with that, 160, 430 and 800 nm PS spheres affected IL-6 and TNF release in human monocyte-derived macrophages at concentrations > 1,000 particles $cell^{-1}$ (Chikaura et al., 2016; Yoshioka et al., 2016). Thus, the limited effects of $PMMA_{polyd.}$ and PS NP in this study is possibly due to lower particle concentrations we used. Moreover, this highlights the importance of improving the comparability of studies by better reporting and aligning particle properties and exposure conditions.

4.3. Why does PVC induce stronger effects than other nanoplastics?

Multiple factors may have caused the strong effects of PVC on cytokine release, including the higher density of PVC, particle-specific morphology and surface chemistry, leachates from the polymer matrix or endotoxin contamination. We excluded the latter by performing a TLR4-inducible NF-κB reporter assay which confirmed that the PVC particles did not contain endotoxins (see S2.9 and S3.6). In addition, $PVC_{polyd.}$ exposure neither cause cytotoxicity (S3.7).

Leaching chemicals from the $PVC_{polyd.}$ particles may have contributed to a small extent to the cytokine release. In MOs, PVC leachates caused a slight but non-significant increase in IL-6 and TNF secretion compared to control. However, the levels were much lower compared to the particle-induced effects. This implies that the chemicals in the NP may have a minor but detectable impact on cytokine release. However, the PVC leachate contained more residual particles than PS and PMMA leachates in which we removed 97 and 99 % of all particles (S3.3). Therefore, we cannot fully differentiate whether the effects of the leachates were induced by chemicals, residual NP or a combination of both. Considering the different magnitudes of effects, the physical toxicity of NP appears to outweigh their chemical toxicity in our study.

One such relevant physical factor causing PVC toxicity could be particle density. Due to its higher density, PVC NP will sink faster according to theoretical calculations (see 3.1) and, thus, cells will be exposed to higher concentrations of PVC compared to the other NP. Based on Stokes' law, up to 58 % of $PVC_{polyd.}$ particles but only 4 % of the irregular $PS_{polyd.}$ NP will be in contact with the cells after 18 h. However, also $PS_{polyd.}$ particles caused some increase in pro-inflammatory cytokine secretion. Hence, other physico-chemical properties may also play a role. Further, the theoretical settling rates for the irregular particles are based on the assumption of monodisperse spherical particles and the resulting exposure ratios must be considered a rough approximation of those of the actual polydisperse NP. In addition, settling rates may be higher if particle agglomeration had occurred and lower if Brownian movement dominates (Gigault et al., 2021). Nevertheless, density is a relevant factor in terms of exposure of attached cells. Thus, better control over and characterization of the actual exposure (e.g., by adjusting concentrations to sinking velocities) is crucial when comparing different NP in future studies (see 4.7).

Different particle morphologies and surface chemistries may also affect the toxicity of NP. While the surface structure of the irregular plastic powders we used is very similar (Fig. S3), their surface charge may be different. In theory, PS, PMMA and PVC all have a negative zeta potential but these can vary between materials and products made of the same polymer (Kirby & Hasselbrink, 2004). As particle uptake by phagocytic immune cell depends on the surface charge (Makino et al., 2003; Yamamoto et al., 2002), differences in surface chemistry may have affected their phagocytosis and, thus, their toxicity. However, cells often do not "see" the bare particle surface but adsorbed biomolecules forming a protein corona (Walczyk et al., 2010). The corona depends on the surface charge and varies with serum type (human/bovine), components and preparation (e.g., heat-inactivation, Lesniak et al., 2010; Lundqvist et al., 2008). In addition, in an environmental setting, chemical pollutants may be adsorbed to the NP surface, a scenario we did not investigate here.

Hence, both the particle surface structure and chemistry as well as protein corona formation may have modulated particle toxicity and are therefore highly relevant properties that need to be investigated more closely in future studies. In conclusion, the facts that PVC NP are more toxic than PMMA and PS particles may be related to differences in density and/or surface chemistry which affect cell-particle interactions.

4.4. Irregular nanoplastics induce stronger effects than spherical ones

Irregular NP induced stronger effects than spherical particles. These results could be due to their rough surface structure. In rats, subcutaneous implantation of irregular PMMA particles produced higher TNF tissue concentrations compared to PMMA nanospheres (Gelb et al., 1994). Here, the authors speculate that the rough surface of the fragmented particles may enhance recognition by and attachment of phagocytotic cells. Furthermore, irregular particles have a larger surface area compared to spherical particles of similar size which increases the relative surface for cell-particle contacts. The higher IL-6 and TNF release triggered by $PS_{polyd.}$, therefore, may be an effect of a stronger interaction of MOs and moDCs with the irregular compared to the spherical particles.

González et al. (1996) previously showed that particle size, surface and volume affect cytokine release. Therefore, the question is whether to compare the effects of different NP based on the particle number, mass, surface area or volume. Currently, there is no consensus in the scientific community on which dose metric to use for NP experiments and previous studies have used any of the four metrics. We decided to keep the particle numbers in our experiment constant as this is a primary measure based on NTA of the stock suspensions. We estimated other dose metrics, including mass-based concentrations, volume and surface area, for better comparison with literature data (see Tab. S2). The use of constant particle numbers, however, results in the different NP used in our study having different surface areas and volumes. While the 50 and 100 nm PS spheres have a much smaller volume and surface area, these metrics are rather similar for the irregular particles and the 310 nm PS spheres. Thus, the effects of the latter NP can be compared keeping the uncertainties in these theoretical estimates in mind (e.g., assumption of spherical particles). Larger NP have a larger total surface that may increase cytokine production (Shanbhag et al., 1995) and will settle faster resulting in a higher exposure. Thus, we expected 310 nm PS spheres to induce stronger effects than the 50 and 100 nm spheres. In contrast, cytokine release does not differ significantly in our experiments with the nanospheres.

This means that either the concentrations of nanospheres in our experiments were too low or that these particles are too small to trigger an immune response. The latter has been observed in previous studies in which nanospheres < 500 nm did not induce inflammatory responses. In human macrophage-like cells exposed to 20–1,000 nm PS nanospheres at a constant mass ratio (i.e., smaller particles were more abundant in terms of number), only 500 and 1,000 nm spheres enhanced IL-6 secretion (Prietl et al., 2014). Similarly, 1,000 nm but not 78 nm PS

spheres increased TNF concentrations in a triple cell culture (epithelial cells, macrophages, DCs) at a constant particle-to-cell ratio (Rothen-Rutishauser et al., 2007). Furthermore, exposure to 5.6 and 9.6 μm PMMA microspheres (1,000 particles cell^{-1}) stimulated IL-6 and TNF release in human monocyte-derived macrophages whereas smaller (160, 430 and 1,600 nm) and larger (19.3 μm) spheres did not (Yoshioka et al., 2016). In contrast, Liu et al. (2015) observed significantly increased TNF and IL-6 release by primary human PBMCs exposed to 60 and 200 nm PS spheres but at exposure concentrations far higher than in this study (approximately 111,000 and 3,000 particles cell^{-1}, recalculated based on the information provided in the reference). In combination with our results, we thus conclude that nanometer-sized plastic spheres (<1 μm) have rather low effects on cytokine release at exposure concentrations of up to 300 NP cell^{-1}

4.5. Effect levels depend on nanoplastic concentrations and cell donors

Concentration-response experiments with $PVC_{polyd.}$ showed that cytokine secretion does not only depend on the applied NP concentration but also on the buffy coat (i.e., the cell donor). A highly variable cytokine release is a frequent constraint in research with primary human immune cells (Chikaura et al., 2016; Matthews et al., 2000). Donor-specific differences may be linked to individual variations in the MO surface receptors which mediate recognition of and interaction with foreign particles (Hamza et al., 2017). Further, the response to NP may also vary distinctively depending on the individual's immune state at the time of blood donation. From this, we conclude that a representative number of buffy coats should be used when investigating the inflammatory effects of particles in primary cells to be able to better assess the inter-individual variability of responses.

4.6. Nanoplastic effects in presence of LPS as second stimulus

LPS, a major compound of the outer cell wall of gram-negative bacteria, caused a strong inflammatory response in moDCs and MOs. LPS binds to the toll-like receptor 4 (TLR4) which actives the NF-kB signaling pathway and regulates inflammatory cytokine signaling (Lu et al., 2008). An additional exposure of LPS-stimulated immune cells with NP did not change the cytokine secretion indicating that NP did not interfere with the activated signaling pathways. These results are in agreement with Prabhu et al. (1998) who exposed murine macrophages to 1–10 μm PMMA particles with (1 μg mL^{-1}) and without LPS. Accordingly, an exposure to NP does not seem to exacerbate already ongoing, pronounced inflammatory processes under the conditions selected for this study. However, the LPS concentrations we used represent a compromise to induce a relatively strong effect on all cytokines. Future experiments with lower concentrations of LPS as well as LPS administration both before and after the treatment can shed light on how NP exposure will modulate the cytokine release under milder inflammatory conditions.

4.7. Limitations and future directions

Our study has a range of limitations that are not uncommon for the emerging field of NP toxicology and provide insights for future studies. We characterized the NP used in this study with regards to their size distribution in physiological saline and their morphology. Nonetheless, other properties are also relevant; for instance, the size of the particles in cell culture medium to characterize their protein corona and potential agglomeration. In addition, information on the surface charge of the NP in cell culture is important to understand potential differences in cell-particle interactions.

Determining the actual NP concentration in contact with cells is important but technically challenging. This is because imaging the settlement of NP is limited by the spatial resolution of the instrument and relies on the particles being fluorescent. Therefore, we calculated theoretical sedimentation rates to estimate the exposure concentrations potentially in contact with the cells, as it is common practice for engineered nanomaterials (Drasler et al., 2017). However, Brownian movement instead of settlement might dominate the distribution of NP in aquatic suspensions (Gigault et al., 2021), rendering such calculations uncertain. Accordingly, new methodological and analytical approaches (e.g., metal-doped NP, Mitrano et al., 2019) are needed to experimentally determine the fate of NP in *in vitro* systems. For certain cell types, also whole blood models or non-adherent systems with rotation might be an applicable alternative to guarantee constant NP-cell interaction.

Alongside the size definition of NP, there is currently no consensus with regards to the appropriate dose metrics to be used in toxicity studies. We used numerical concentrations based on our NTA results and estimated mass-based, volumetric and surface area-based concentrations from these. While the latter were comparable for the larger NP, such estimates are uncertain due to the assumptions we had to make. The question of which dose metric is indeed most appropriate can only be answered by studies that elucidate the mechanisms by which NP contact induces an inflammatory response. Similar to the recommendations for engineered nanomaterials (Drasler et al., 2017), reporting multiple dose metrics is the best way to ensure comparability between studies until robust mechanistic knowledge is available.

Finally, we used LPS as positive control because it represents a common standard and potent trigger of inflammation in various immune cells. Since LPS probably triggers cytokine induction by another mechanism than plastic particles (LPS activates toll-like receptor 4, which our NP did not), using reference particles in addition to LPS is desirable to put the toxicity of NP in context. However, finding appropriate non-plastic particles that closely match the physico-chemical properties of NP is difficult. One way forward is related to a better mechanistic understanding of how NP induce inflammation. This could be achieved by performing targeted approaches analyzing activated cellular sensors and signaling mechanisms. This would enable designing reference materials that trigger the same mechanisms and comparing the toxicity between particles and studies.

5. Conclusion

Our study illustrates that NP exposure induces the secretion of pro- and anti-inflammatory cytokines in primary human monocytes and dendritic cells. In our experiments, the cytokine release especially depends on the polymer type with irregular, polydisperse PVC particles inducing stronger effects compared to irregular polydisperse PMMA and PS NP. Likewise, the shape of the NP is a relevant factor with irregular PS NP inducing a stronger response than spherical PS NP. Thus, NP cannot be considered one homogenous entity when assessing their toxicity and using commercially available PS beads might underestimate the inflammatory effects of other NP. While the chemicals leaching from the particles had limited effects, the cytokine response to NP exposures varies between the individual buffy coats and donors. This points towards different individual susceptibilities to NP exposure and highlights the need to use an appropriate sample size when working with primary human cells.

Acknowledging the limitations of our study (see above), we conclude that NP can trigger inflammatory responses in human immune cells. Due to the lack of knowledge on the actual human exposure to NP, it is, however, impossible to determine whether the NP concentrations we used adequately reflect internal levels, limiting our ability to extrapolate from *in vitro* to *in vivo* and to draw further conclusions on the health risks of NP. To assess the latter, we need to better understand their toxicokinetics, the actual levels of human exposure, and their toxicological effects considering differences in immunological status (challenges of infection, cancer).

Declaration of Competing Interest

The authors declare the following financial interests/personal relationships which may be considered as potential competing interests: MW is an unremunerated member of the Scientific Advisory Board of Food Packaging Forum and has received travel funding to attend annual board meetings. The other authors declare no potential competing interests.

Acknowledgements

Author contributions

AW conceived the study; AW, AS, MW, BR and HHR discussed the study design, its implementation and the results; AW, AS and BR performed the main experiments; HS, JS and AMN optimized and performed the TLR4/NF-κB reporter assay, AW analyzed the data; AW, MW and BR wrote the manuscript; all authors commented on the manuscript.

Credits

We gratefully acknowledge the support of Prof. Dr. Jörg Oehlmann for providing infrastructure for the study. We thank Martina Herrero San Juan, Katrin Jurida and Andrea Janicova for assistance throughout the cell culture experiments as well as Georg Dierkes for performing the py–GC–MS analysis. Furthermore, we thank Michael Göbel and his group for supporting the ATR–FTIR analysis and Robert Tampé and his group for supporting NanoSight analysis.

Funding

AW was funded by the German Federal Ministry of Transport and Digital Infrastructure. AS and HHR were supported by the Deutsche Forschungsgemeinschaft (DFG grant number: SFB1039/B03) awarded to HHR. JS was funded by a grant from the Research Council of Norway Grant 223255/F50 through its Centers of Excellence funding scheme.

Appendix A. Supplementary material

Supplementary data to this article can be found online at https://doi.org/10.1016/j.envint.2022.107173.

References

Arlt, O., Schwiebs, A., Japtok, L., Rüger, K., Katzy, E., Kleuser, B., Radeke, H.H., 2014. Sphingosine-1-phosphate modulates dendritic cell function: focus on non-migratory effects in vitro and in vivo. Cell. Physiol. Biochem. 34 (1), 27–44. https://doi.org/10.1159/000362982.

Barboza, L.G.A., Dick Vethaak, A., Lavorante, B.R.B.O., Lundebye, A.-K., Guilhermino, L., 2018. Marine microplastic debris: An emerging issue for food security, food safety and human health. Mar. Pollut. Bull. 133, 336–348. https://doi.org/10.1016/j.marpolbul.2018.05.047.

Carr, K.E., Hazzard, R.A., Reid, S., Hodges, G.M., 1996. The effect of size on uptake of orally administered latex microparticles in the small intestine and transport to mesenteric lymph nodes. Pharm. Res. 13 (8), 1205–1209. https://doi.org/10.1023/a:1016064320334.

Chadha, H.S., Wooley, P.H., Sud, S., Fitzgerald, R.H., 1995. Cellular proliferation and cytokine responses to polymethylmethacrylate particles in patients with a cemented total joint arthroplasty. Inflamm. Res. 44 (4), 145–151. https://doi.org/10.1007/BF01782811.

Chikaura, H., Nakashima, Y., Fujiwara, Y., Komohara, Y., Takeya, M., Nakanishi, Y., 2016. Effect of particle size on biological response by human monocyte-derived macrophages. Biosurf. Biotribol. 2 (1), 18–25. https://doi.org/10.1016/j.bsbt.2016.02.003.

Cox, K.D., Covernton, G.A., Davies, H.L., Dower, J.F., Juanes, F., Dudas, S.E., 2019. Human consumption of microplastics. Environ. Sci. Technol. 53 (12), 7068–7074. https://doi.org/10.1021/acs.est.9b01517.

Danopoulos, E., Twiddy, M., West, R., Rotchell, J.M., 2021. A rapid review and meta-regression analyses of the toxicological impacts of microplastic exposure in human cells. J. Hazard. Mater. 427, 127861 https://doi.org/10.1016/j.jhazmat.2021.127861.

Drasler, B., Sayre, P., Steinhäuser, K.G., Petri-Fink, A., Rothen-Rutishauser, B., 2017. In vitro approaches to assess the hazard of nanomaterials. NanoImpact 8, 99–116. https://doi.org/10.1016/j.impact.2017.08.002.

Dris, R., Gasperi, J., Mirande, C., Mandin, C., Guerrouache, M., Langlois, V., Tassin, B., 2017. A first overview of textile fibers, including microplastics, in indoor and outdoor environments. Environ. Pollut. 221, 453–458. https://doi.org/10.1016/j.envpol.2016.12.013.

Foged, C., Brodin, B., Frokjaer, S., Sundblad, A., 2005. Particle size and surface charge affect particle uptake by human dendritic cells in an in vitro model. Int. J. Pharm. 298 (2), 315–322. https://doi.org/10.1016/j.ijpharm.2005.03.035.

Gelb, H., Schumacher, H.R., Cuckler, J., Ducheyne, P., Baker, D.G., 1994. In vivo inflammatory response to polymethylmethacrylate particulate debris: effect of size, morphology, and surface area. J. Orthop. Res. 12 (1), 83–92. https://doi.org/10.1002/jor.1100120111.

Gibon, E., Córdova, L.A., Lu, L., Lin, T.-H., Yao, Z., Hamadouche, M., Goodman, S.B., 2017. The biological response to orthopedic implants for joint replacement. II: Polyethylene, ceramics, PMMA, and the foreign body reaction. J. Biomed. Mater. Res. Part B 105 (6), 1685–1691. https://doi.org/10.1002/jbm.b.33676.

Gigault, J., El Hadri, H., Nguyen, B., Grassl, B., Rowenczyk, L., Tufenkji, N., Feng, S., Wiesner, M., 2021. Nanoplastics are neither microplastics nor engineered nanoparticles. Nat. Nanotechnol. 16 (5), 501–507. https://doi.org/10.1038/s41565-021-00886-4.

González, O., Smith, R.L., Goodman, S.B., 1996. Effect of size, concentration, surface area, and volume of polymethylmethacrylate particles on human macrophagesin vitro. J. Biomed. Mater. Res. 30 (4), 463–473. https://doi.org/10.1002/(SICI)1097-4636(199604)30:4<463::AID-JBM4>3.0.CO;2-N.

Goodman, S., Lidgren, L., 1992. Polyethylene wear in knee arthroplasty. A review. Acta Orthopaedica Scandinavica 63 (3), 358–364. https://doi.org/10.3109/17453679209154804.

Hamza, E., Kittl, S., & Kuhnert, P. (2017). Temporal induction of pro-inflammatory and regulatory cytokines in human peripheral blood mononuclear cells by Campylobacter jejuni and Campylobacter coli. PloS One, 12(2), e0171350. 10.1371/journal.pone.0171350.

Han, S., Bang, J., Choi, D., Hwang, J., Kim, T., Oh, Y., Hwang, Y., Choi, J., Hong, J., 2020. Surface pattern analysis of microplastics and their impact on human-derived cells. ACS Applied Polymer Materials 2 (11), 4541–4550. https://doi.org/10.1021/acsapm.0c00645.

Harmsen, A.G., Muggenburg, B.A., Snipes, M.B., Bice, D.E., 1985. The role of macrophages in particle translocation from lungs to lymph nodes. Science 230 (4731), 1277–1280. https://doi.org/10.1126/science.4071052.

Hartmann, N.B., Hüffer, T., Thompson, R.C., Hassellöv, M., Verschoor, A., Daugaard, A. E., Rist, S., Karlsson, T., Brennholt, N., Cole, M., Herrling, M.P., Hess, M.C., Ivleva, N. P., Lusher, A.L., Wagner, M., 2019. Are we speaking the same language? Recommendations for a definition and categorization framework for plastic debris. Environ. Sci. Technol. 53 (3), 1039–1047. https://doi.org/10.1021/acs.est.8b05297.

Hinderliter, P.M., Minard, K.R., Orr, G., Chrisler, W.B., Thrall, B.D., Pounds, J.G., Teeguarden, J.G., 2010. ISDD: A computational model of particle sedimentation, diffusion and target cell dosimetry for in vitro toxicity studies. Part. Fibre Toxicol. 7 (1), 36. https://doi.org/10.1186/1743-8977-7-36.

Horowitz, S.M., Doty, S.B., Lane, J.M., Burstein, A.H., 1993. Studies of the mechanism by which the mechanical failure of polymethylmethacrylate leads to bone resorption. J. Bone Joint Surg. American 75 (6), 802–813. https://doi.org/10.2106/00004623-199306000-00002.

Huaux, F., 2018. Emerging role of immunosuppression in diseases induced by micro- and nano-particles: Time to revisit the exclusive inflammatory scenario. Front. Immunol. 9, 2364. https://doi.org/10.3389/fimmu.2018.02364.

Hwang, J., Choi, D., Han, S., Jung, S.Y., Choi, J., Hong, J., 2020. Potential toxicity of polystyrene microplastic particles. Sci. Rep. 10 (1), 7391. https://doi.org/10.1038/s41598-020-64464-9.

Ingham, E., Fisher, J., 2000. Biological reactions to wear debris in total joint replacement. Proc. Inst. Mech. Eng. Part H. 214 (1), 21–37. https://doi.org/10.1243/0954411001535219.

Kawecki, D., Nowack, B., 2019. Polymer-specific modeling of the environmental emissions of seven commodity plastics as macro- and microplastics. Environ. Sci. Technol. 53 (16), 9664–9676. https://doi.org/10.1021/acs.est.9b02900.

Kiama, S.G., Cochand, L., Karlsson, L., Nicod, L.P., Gehr, P., 2001. Evaluation of phagocytic activity in human monocyte-derived dendritic cells. J. Aerosol Med. 14 (3), 289–299. https://doi.org/10.1089/089426801316970240.

Kirby, B.J., Hasselbrink, E.F., 2004. Zeta potential of microfluidic substrates: 2 Data for polymers. ELECTROPHORESIS 25 (2), 203–213. https://doi.org/10.1002/elps.200305755.

Kohli, A.K., Alpar, H.O., 2004. Potential use of nanoparticles for transcutaneous vaccine delivery: effect of particle size and charge. Int. J. Pharm. 275 (1–2), 13–17. https://doi.org/10.1016/j.ijpharm.2003.10.038.

Kramm, J., Völker, C., Wagner, M., 2018. Superficial or substantial: Why care about microplastics in the anthropocene? Environ. Sci. Technol. 52 (6), 3336–3337. https://doi.org/10.1021/acs.est.8b00790.

Lambert, S., Wagner, M., 2016. Formation of microscopic particles during the degradation of different polymers. Chemosphere 161, 510–517. https://doi.org/10.1016/j.chemosphere.2016.07.042.

Lesniak, A., Campbell, A., Monopoli, M.P., Lynch, I., Salvati, A., Dawson, K.A., 2010. Serum heat inactivation affects protein corona composition and nanoparticle uptake. Biomaterials 31 (36), 9511–9518. https://doi.org/10.1016/j.biomaterials.2010.09.049.

Lind, M., Trindade, M.C.D., Yaszay, B., Goodman, S.B., Smith, R.L., 1998. Effects of particulate debris on macrophage-dependent fibroblast stimulation in coculture. The Journal of Bone and Joint Surgery. British Volume. 80 (5), 924–930. https://doi.org/10.1302/0301-620x.80b5.8710.

Liu, A., Richards, L., Bladen, C.L., Ingham, E., Fisher, J., Tipper, J.L., 2015. The biological response to nanometre-sized polymer particles. Acta Biomater. 23, 38–51. https://doi.org/10.1016/j.actbio.2015.05.016.

Lu, Y.-C., Yeh, W.-C., Ohashi, P.S., 2008. LPS/TLR4 signal transduction pathway. Cytokine 42 (2), 145–151. https://doi.org/10.1016/j.cyto.2008.01.006.

Lundqvist, M., Stigler, J., Elia, G., Lynch, I., Cedervall, T., Dawson, K.A., 2008. Nanoparticle size and surface properties determine the protein corona with possible implications for biological impacts. Proc. Natl. Acad. Sci. 105 (38), 14265–14270. https://doi.org/10.1073/pnas.0805135105.

Mahe, B., Vogt, A., Liard, C., Duffy, D., Abadie, V., Bonduelle, O., Boissonnas, A., Sterry, W., Verrier, B., Blume-Peytavi, U., Combadiere, B., 2009. Nanoparticle-based targeting of vaccine compounds to skin antigen-presenting cells by hair follicles and their transport in mice. J. Invest. Dermatol. 129 (5), 1156–1164. https://doi.org/10.1038/jid.2008.356.

Makino, K., Yamamoto, N., Higuchi, K., Harada, N., Ohshima, H., Terada, H., 2003. Phagocytic uptake of polystyrene microspheres by alveolar macrophages: effects of the size and surface properties of the microspheres. Colloids Surf., B 27 (1), 33–39. https://doi.org/10.1016/S0927-7765(02)00042-5.

Marchant, R.E., Anderson, J.M., Dillingham, E.O., 1986. In vivo biocompatibility studies. VII. Inflammatory response to polyethylene and to a cytotoxic polyvinylchloride. J. Biomed. Mater. Res. 20 (1), 37–50. https://doi.org/10.1002/jbm.820200105.

Matthews, J.B., Besong, A.A., Green, T.R., Stone, M.H., Wroblewski, B.M., Fisher, J., Ingham, E., 2000. Evaluation of the response of primary human peripheral blood mononuclear phagocytes to challenge within vitro generated clinically relevant UHMWPE particles of known size and dose. J. Biomed. Mater. Res. 52 (2), 296–307. https://doi.org/10.1002/1097-4636(200011)52:2<296::aid-jbm8>3.0.co;2-9.

Mitrano, D.M., Beltzung, A., Frehland, S., Schmiedgruber, M., Cingolani, A., Schmidt, F., 2019. Synthesis of metal-doped nanoplastics and their utility to investigate fate and behaviour in complex environmental systems. Nat. Nanotechnol. 14 (4), 362–368. https://doi.org/10.1038/s41565-018-0360-3.

Nakashima, Y., Sun, D.H., Trindade, M.C.D., Chun, L.E., Song, Y., Goodman, S.B., Schurman, D.J., Maloney, W.J., Smith, R.L., 1999. Induction of macrophage C-C chemokine expression by titanium alloy and bone cement particles. The Journal of Bone and Joint Surgery. British Volume. 81 (1), 155–162. https://doi.org/10.1302/0301-620x.81b1.8884.

Norwegian Scientific Committee for Food and Environment. (2019). Microplastics; occurrence, levels and implications for environment and human health related to food. Opinion of the Steering Committee of the Norwegian Scientific Committee for Food and Environment. (No. 16). Oslo, Norway. https://vkm.no/english/riskassessments/riskassesments.4.2375207615dac0245ae7444e.html?s=publisert.

Pigott, G.H., Ishmael, J., 1979. A comparison between in vitro toxicity of PVC powders and their tissue reaction in vivo. The Annals of Occupational Hygiene 22 (2), 111–126. https://doi.org/10.1093/annhyg/22.2.111.

Prabhu, A., Shelburne, C.E., Gibbons, D.F., 1998. Cellular proliferation and cytokine responses of murine macrophage cell line J774A.1 to polymethylmethacrylate and cobalt-chrome alloy particles. J. Biomed. Mater. Res. 42 (4), 655–663. https://doi.org/10.1002/(sici)1097-4636(19981215)42:4<655::aid-jbm23>3.0.co;2-b.

Prata, J.C., 2018. Airborne microplastics: Consequences to human health? Environ. Pollut. 234, 115–126. https://doi.org/10.1016/j.envpol.2017.11.043.

Prietl, B., Meindl, C., Roblegg, E., Pieber, T.R., Lanzer, G., Fröhlich, E., 2014. Nano-sized and micro-sized polystyrene particles affect phagocyte function. Cell Biol. Toxicol. 30 (1), 1–16. https://doi.org/10.1007/s10565-013-9265-y.

Rinker, K.D., Prabhakar, V., Truskey, G.A., 2001. Effect of contact time and force on monocyte adhesion to vascular endothelium. Biophys. J . 80 (4), 1722–1732. https://doi.org/10.1016/S0006-3495(01)76143-7.

Rothen-Rutishauser, B., Mühlfeld, C., Blank, F., Musso, C., Gehr, P., 2007. Translocation of particles and inflammatory responses after exposure to fine particles and nanoparticles in an epithelial airway model. Part. Fibre Toxicol. 4 (1), 9. https://doi.org/10.1186/1743-8977-4-9.

SAPEA, Science Advice for Policy by European Academies. (2018). A Scientific Perspective on Microplastics in Nature and Society. Berlin. https://www.sapea.info/topics/microplastics/ 10.26356/microplastics.

Schmalzried, T.P., Jasty, M., Harris, W.H., 1992. Periprosthetic bone loss in total hip arthroplasty. Polyethylene wear debris and the concept of the effective joint space. The Journal of Bone and Joint Surgery. American 74 (6), 849–863.

Shanbhag, A.S., Jacobs, J.J., Black, J., Galante, J.O., Glant, T.T., 1995. Human monocyte response to particulate biomaterials generated in vivo and in vitro. J. Orthop. Res. 13 (5), 792–801. https://doi.org/10.1002/jor.1100130520.

Snipes, M.B., Chavez, G.T., Muggenburg, B.A., 1984. Disposition of 3-, 7-, and 13-μm microspheres instilled into lungs of dogs. Environ. Res. 33 (2), 333–342. https://doi.org/10.1016/0013-9351(84)90031-8.

Tada, Y., Koarada, S., Morito, F., Mitamura, M., Inoue, H., Suematsu, R., Ohta, A., Miyake, K., Nagasawa, K., 2008. Toll-like receptor homolog RP105 modulates the antigen-presenting cell function and regulates the development of collagen-induced arthritis. Arthritis Research & Therapy 10 (5), R121. https://doi.org/10.1186/ar2529.

Teh, Y.C., Ding, J.L., Ng, L.G., Chong, S.Z., 2019. Capturing the fantastic voyage of monocytes through time and space. Front. Immunol. 10, 834. https://doi.org/10.3389/fimmu.2019.00834.

Trindade, M.C.D., Lind, M., Goodman, S.B., Maloney, W.J., Schurman, D.J., Smith, R.L., 1999. Interferon-gamma exacerbates polymethylmethacrylate particle-induced interleukin-6 release by human monocyte/macrophagesin vitro. J. Biomed. Mater. Res. 47 (1), 1–7. https://doi.org/10.1002/(sici)1097-4636(199910)47:1<1::aid-jbm1>3.0.co;2-8.

Trindade, M.C.D., Lind, M., Nakashima, Y., Sun, D.H., Goodman, S.B., Schurman, D.J., Smith, R.L., 2001. Interleukin-10 inhibits polymethylmethacrylate particle induced interleukin-6 and tumor necrosis factor-α release by human monocyte/macrophages in vitro. Biomaterials 22 (15), 2067–2073. https://doi.org/10.1016/s0142-9612(00)00376-8.

de Waal Malefyt, R., Abrams, J., Bennett, B., Figdor, C.G., de Vries, J.E., 1991. Interleukin 10(IL-10) inhibits cytokine synthesis by human monocytes: an autoregulatory role of IL-10 produced by monocytes. J. Exp. Med. 174 (5), 1209–1220. https://doi.org/10.1084/jem.174.5.1209.

Wagner, S., Reemtsma, T., 2019. Things we know and don't know about nanoplastic in the environment. Nat. Nanotechnol. 14 (4), 300–301. https://doi.org/10.1038/s41565-019-0424-z.

Waisman, A., Lukas, D., Clausen, B.E., Yogev, N., 2017. Dendritic cells as gatekeepers of tolerance. Semin. Immunopathol. 39 (2), 153–163. https://doi.org/10.1007/s00281-016-0583-z.

Walczyk, D., Bombelli, F.B., Monopoli, M.P., Lynch, I., Dawson, K.A., 2010. What the cell "sees" in bionanoscience. J. Am. Chem. Soc. 132 (16), 5761–5768. https://doi.org/10.1021/ja910675v.

Wooley, P.H., Nasser, S., Fitzgerald, R.H., 1996. The immune response to implant materials in humans. Clinical Orthopaedics and Related Research 326, 63–70. https://doi.org/10.1097/00003086-199605000-00008.

Wright, S.L., Kelly, F.J., 2017. Plastic and human health: A micro issue? Environ. Sci. Technol. 51 (12), 6634–6647. https://doi.org/10.1021/acs.est.7b00423.

Yamamoto, N., Fukai, F., Ohshima, H., Terada, H., Makino, K., 2002. Dependence of the phagocytic uptake of polystyrene microspheres by differentiated HL60 upon the size and surface properties of the microspheres. Colloids Surf., B 25 (2), 157–162. https://doi.org/10.1016/S0927-7765(01)00306-X.

Yoshioka, R., Nakashima, Y., Fujiwara, Y., Komohara, Y., Takeya, M., Nakanishi, Y., 2016. The biological response of macrophages to PMMA particles with different morphology and size. Biosurf. Biotribol. 2 (3), 114–120. https://doi.org/10.1016/j.bsbt.2016.09.003.

Zimmermann, L., Dierkes, G., Ternes, T.A., Völker, C., Wagner, M., 2019. Benchmarking the in vitro toxicity and chemical composition of plastic consumer products. Environ. Sci. Technol. 53 (19), 11467–11477. https://doi.org/10.1021/acs.est.9b02293.